

1-1-2006

Peculiarities of the Electric and Thermoelectric Properties of GaTe

M. M. NASSARY

Follow this and additional works at: <https://journals.tubitak.gov.tr/physics>



Part of the [Physics Commons](#)

Recommended Citation

NASSARY, M. M. (2006) "Peculiarities of the Electric and Thermoelectric Properties of GaTe," *Turkish Journal of Physics*: Vol. 30: No. 2, Article 4. Available at: <https://journals.tubitak.gov.tr/physics/vol30/iss2/4>

This Article is brought to you for free and open access by TÜBİTAK Academic Journals. It has been accepted for inclusion in Turkish Journal of Physics by an authorized editor of TÜBİTAK Academic Journals. For more information, please contact academic.publications@tubitak.gov.tr.

Peculiarities of the Electric and Thermoelectric Properties of GaTe

M. M. NASSARY

*Department of Physics, Faculty of Science, South Valley University,
Qena-EGYPT
e-mail: Nassary_99@Yahoo.com*

Received 18.05.2005

Abstract

Measurements of electrical conductivity, Hall coefficient and thermoelectric power were carried out over the temperature range 136–563 K for GaTe compound grown in single crystal form by modified Bridgman technique. The crystals obtained had Positive-type conductivity with a hole concentration of $3.8 \times 10^{12} \text{ cm}^{-3}$ at room temperature. Conductivity and Hall mobility at room temperature were evaluated as $4.4 \times 10^{-3} \text{ ohm}^{-1} \text{ cm}^{-1}$ and $7079 \text{ cm}^2/\text{V}\cdot\text{s}$, respectively. The energy gap width of 1.5 eV was found. The effective mass of holes and electrons at room temperature were $4.16 m_0$ and $0.1174 m_0$, respectively

Key Words: GaTe, Electrical conductivity, Thermoelectric power.

1. Introduction

Among III-VI group semiconductors, GaTe has a particular place for its interesting physical properties. Gallium-Tellurium is a binary alloy system that exhibits anomalous physical and chemical properties [1]. Layered semiconductors have been of interest recently for their possible applications in devices exhibiting Van der Waals epitaxy [2]. III-VI compounds such as GaSe and GaTe are also formed as intermediate layers during the epitaxial growth of II-VI on III-V compounds [3]. As in other better known III-VI layered semiconductors, bonds inside the layers are mainly covalent [4, 5]. Every Ga atom is surrounded by three Te atoms and one Ga atom, in quasi-tetrahedral coordination. The layers are bound mainly by Van der Waals forces between Te atoms. Unlike GaS or GaSe, in which all Ga-Ga bonds are perpendicular to the layers, in GaTe one third of the Ga-Ga bonds are parallel to the layers, giving rise to a supplementary cleaving plane along the *c*-axis, so that the crystals can be very easily oriented. Most published works presented in the literature have been concerned with the measurement of electrical properties [6–11], optical properties [12–16], structural properties [17, 18] and photoluminescence characterization [19].

2. Experimental

In order to grow perfect GaTe Single Crystal, a modified Bridgman-Stockbarger technique was used [20]. The ampoule is charged with equimolar 5N Gallium and 5N Tellurium. The appropriate amount was first sealed in silica ampoule at a pressure of 10^{-5} Torr. As the growth run began, the ampoule was held in

the hot zone of the furnace at 1180 K for about 24 hours for melt homogenization. Several times during heating the melt was shaken to accelerate the co-diffusion of the constituents. The mechanical system is always used to draw the charged ampoule from one zone to another with the required rate. In our case, the charged ampoule is lowered gradually and slowly through temperature steps at a rate of about 1.6 mm/h. The temperature of the middle zone is 1121 K corresponding to the crystallization temperature of GaTe according to the phase diagram [21]. The duration time for producing GaTe as single crystal is about eleven days. The grown GaTe was in crystal form as identified from x-ray diffraction analysis.

To study the electrical conductivity and Hall effect, the sample was prepared in a rectangular shape with dimensions $9.75 \times 4 \times 2.6 \text{ mm}^3$. Silver paste was used to form ohmic contacts. Measured current-voltage characteristics confirmed the ohmic nature of the contacts. The conductivity and the Hall coefficient were measured by a compensation method in a special cryostat [22] under a 0.5 Tesla magnetic field with a conventional dc type UJ 33E Mark potentiometer. The temperature range of investigation was between 136 K up to 563 K. All measurements were carried out under vacuum of about 10^{-3} Torr.

To study the thermoelectric power (TEP) of the samples, an evacuated calorimeter at 10^{-3} Torr was used to protect the sample from oxidation and water vapor condensation at all temperatures. The calorimeter has two heaters. The outer heater (the external source) discharges its heat slowly to the specimen environment. The inner heater (connected to the lower end of the crystal) was made purposely to control the temperature and its gradient along the specimen. The TEP is calculated at different temperatures by dividing the magnitude of the thermo-voltage difference across the crystal by the temperature difference between the hot and cold ends.

3. Results and Discussion

3.1. Temperature dependence of electrical conductivity and Hall effect for GaTe

Electrical properties of GaTe in a crystalline form and their temperature dependence were investigated over the wide temperature range 136–563 K. Figure 1 shows the results for electrical conductivity as a function of temperature. The curve consists of three regions. The first region lies is 136–384 K and represents the extrinsic region. In this region, the conductivity was observed to increase with temperature, indicating that impurity atoms are ionized under the influence of temperature at this stage. From the slope of the curve in this region, the ionization energy was evaluated to $E_a = 0.26 \text{ eV}$. The second region lies over the temperature range 384–500 K, and indicates the transition region. The third region lies at 500–563 K, is the intrinsic part. Here the conductivity increased with temperature due to the excitation of carriers from the valence band to the conduction band. From the slope of the curve in this region, the energy gap is calculated at $E_g = 1.5 \text{ eV}$. This value is close to values obtained from previous measurements [8, 14, 23]. The conductivity at room temperature is evaluated as $\sigma = 4.4 \times 10^{-3} \text{ ohm}^{-1} \text{ cm}^{-1}$. The investigated sample turned out to be p-type in the whole temperature range, in agreement with previous works [6, 9].

Figure 2 shows the relationship between $R_H T^{3/2}$ and $10^3/T$ where R_H is the Hall coefficient and T is the absolute temperature. This curve also consists of three regions. The first region lies in the temperature range 163–384 K, and corresponds to the extrinsic region. Therefore, from the behavior shown here, we calculated the ionization energy to be $E_a = 0.24 \text{ eV}$. The second region, which lies between 384–500 K, indicates the transition region. The third region that lies between 500–563 K, and indicates the intrinsic region. From this latter part we calculated the energy gap to be $E_g = 1.51 \text{ eV}$. These results in a good agreement with those obtained from the conductivity measurements.

Figure 3 show the relation between Hall mobility and temperature. The Hall mobility is deduced from the relation $\mu_H = R_H \sigma$. In this figure, the mobility decreases linearly with increasing temperature according to the law $\mu \propto T^{-1.2}$. The scattering mechanism is thermal lattice scattering, and dominates this case. These results agreed with the previous work [11]. At room temperature Hall mobility is equal to 7079

$\text{cm}^2/\text{V}\cdot\text{s}$. The relation between carrier concentration and temperature is illustrated in Figure 4. From an intrinsic and extrinsic region, we calculated the energy gap and ionization energy $E_g = 1.51 \text{ eV}$, $E_a = 0.24 \text{ eV}$, respectively. These values are found to be in a good agreement with the above values. The carrier concentration at room temperature calculated to be $3.8 \times 10^{12} \text{ cm}^{-3}$.

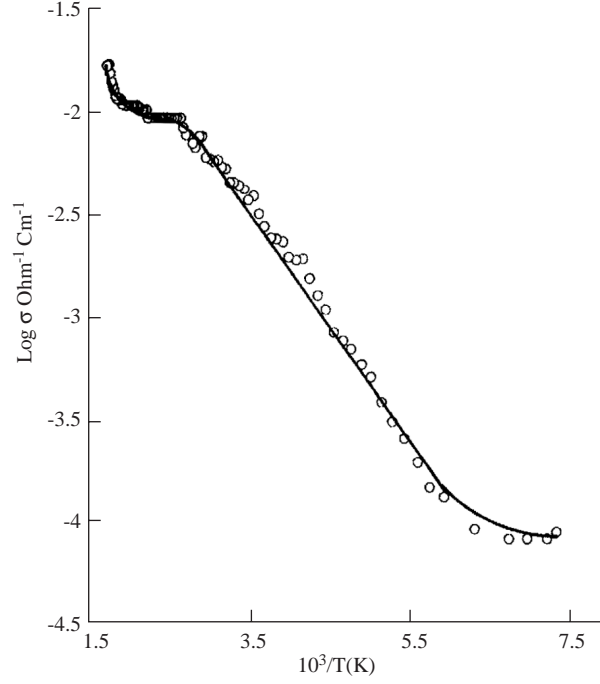


Figure 1. Temperature dependence of the electrical conductivity for GaTe single crystal.

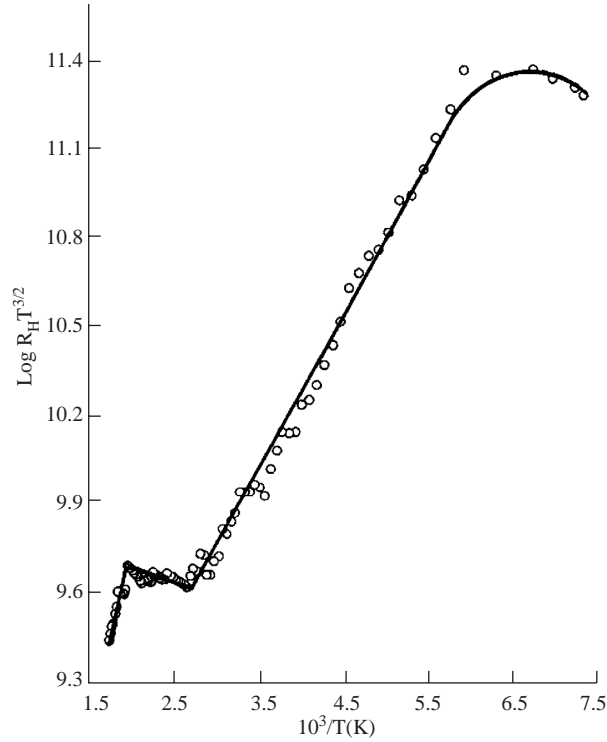


Figure 2. Relation between $R_H T^{3/2}$ and $10^3/T$ for GaTe single crystal.

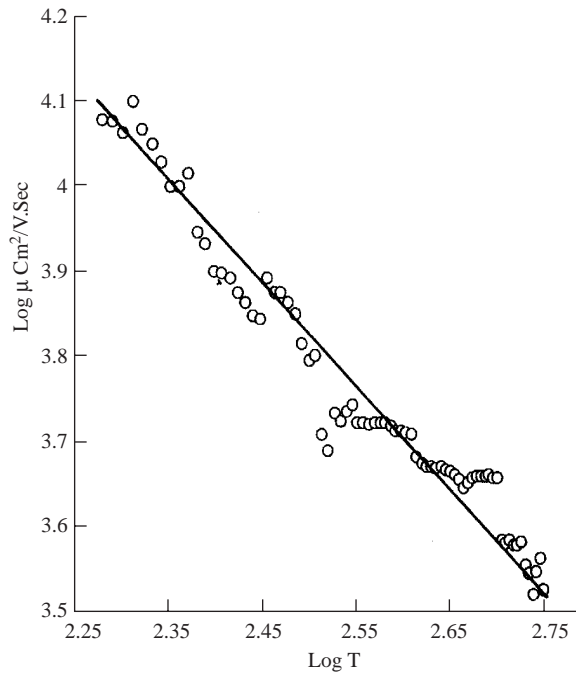


Figure 3. The behavior of Hall mobility as a function of temperature for GaTe single crystal.

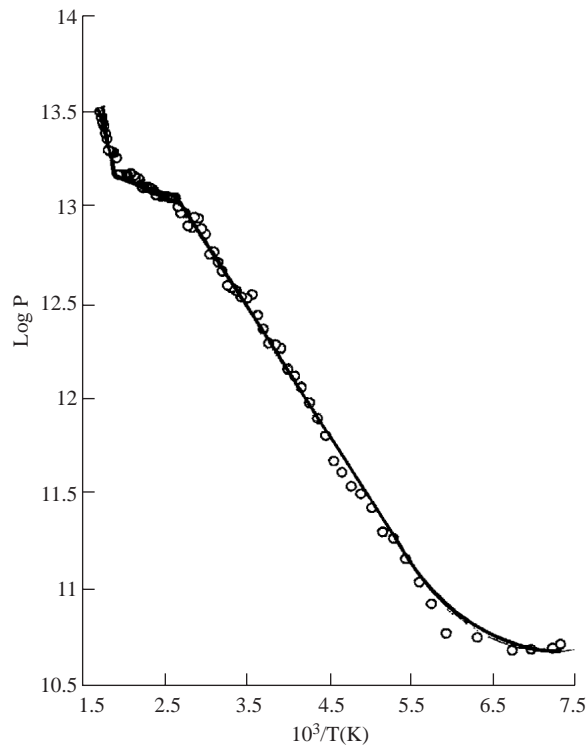


Figure 4. Variation of holes concentration with temperature for GaTe Single crystal.

3.2. Temperature dependence of thermoelectric power for GaTe

The thermoelectric power for GaTe was characterized in the temperature range 180–503 K and is shown in Figure 5. At the beginning of the curve TEP increases with temperature, reaching a maximum value at $\alpha =$

558.5 $\mu\text{V}/\text{K}$, corresponding to the temperature 463 K. We know the thermoelectric power can be expressed as a sum of two contributions: the electronic part and the phonon contribution known as the phonon drag thermoelectric power. It is our understanding that the high value of TEP in high temperature range is due to the electronic part. Beyond this point, the value of TEP decreases linearly with increasing temperature. This behavior is in good agreement to the previous work [7]. The room temperature thermoelectric power value is found to be 124 $\mu\text{V}/\text{K}$. The results show that, the conduction can be regarded as p-type over the whole temperature range.

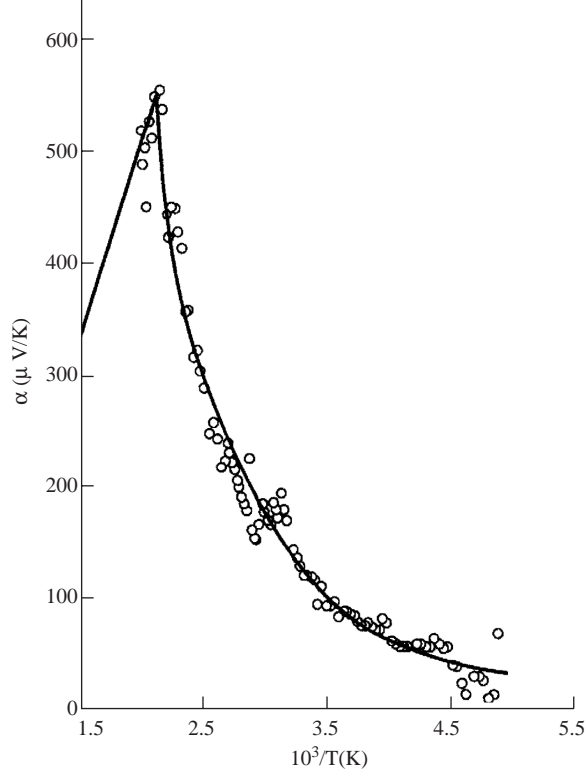


Figure 5. Relation between α and $10^3/T$ for GaTe single crystal.

The behavior of thermoelectric power with temperature in the intrinsic region can be described by the equation [24]

$$\alpha = -\frac{K}{e} \left[\frac{b-1}{b+1} \left(\frac{E_g}{2KT} + 2 \right) + \frac{1}{2} \text{Ln} \left(\frac{m_n^*}{m_p^*} \right)^{3/2} \right], \quad (1)$$

where, b is the ratio of electron and hole mobility, E_g is the energy gap and (m_n^*, m_p^*) are the effective mass of electrons and holes, respectively. The relationship shows that a plot of α in the intrinsic range as a function of the reciprocal of absolute temperature is straight line as shown in Figure 5. The slope of the linear part is used to estimate the ratio of the electron and hole mobility. Taking $E_g = 1.51$ eV, the ratio $b = \frac{\mu_n}{\mu_p}$ is found to be 2.6. Hence by using the value of $\mu_p = 7079$ $\text{cm}^2/\text{V}\cdot\text{s}$, the electron mobility can be deduced and its value is found to be 18405 $\text{cm}^2/\text{V}\cdot\text{s}$.

Another important parameter can be deduced with the aid of the obtained values μ_n and μ_p using the famous Einstein relation that is the diffusion coefficient for both carriers (holes and electrons) can be evaluated to be 176.9 and 460.1 cm^2/s , respectively. From the intersection of the curve, the ratio between the effective masses of electrons and holes can be estimated to be $m_n^*/m_p^* = 0.028$.

In the impurity region the following equation can be applied [25]:

$$\alpha = \frac{K}{e} \left[2 - Ln \frac{ph^3}{2(2\pi m_p^*KT)^{3/2}} \right] \quad (2)$$

The effective mass of holes m_p^* is calculated from the relation between thermoelectric power and $\ln p$. The relation is illustrated in Figure 6. Note that α increases exponentially with increase in carrier concentration. Calculation of the effective mass of holes from the intersection of the curve yields the value $m_p^* = 4.16 m_o$. Combining these values with the above mentioned results for the ratio $\frac{m_n^*}{m_p^*}$ one obtains an effective mass of electrons as $m_n^* = 0.1174 m_o$. The results indicate that the electron mobility is much higher than the hole mobility. This is acceptable since the hole effective mass is much greater than that of electrons. The calculated values of the effective masses for both minority and majority carriers can be used for the determination of the relaxation time for both current carriers. Its value for holes comes to be 1.24×10^{-13} s, whereas for electrons 9.12×10^{-16} s. Also the diffusion length $L = \sqrt{D\tau}$, the values of L_p, L_n are calculated and it is found to be 4.09×10^{-6} cm and 6.8×10^{-7} cm for holes and electrons, respectively. Figure 7 shows the dependence of thermoelectric power coefficient α on the natural logarithm of electrical conductivity according to [26]:

$$\alpha = \frac{K}{e} \left[A + \ln \frac{2(2\pi m_p^*KT)^{3/2}e\mu}{(2\pi h)^3} \right] - \frac{K}{e} Ln\sigma \quad (3)$$

It seems that the TEP increased with decreasing conductivity.

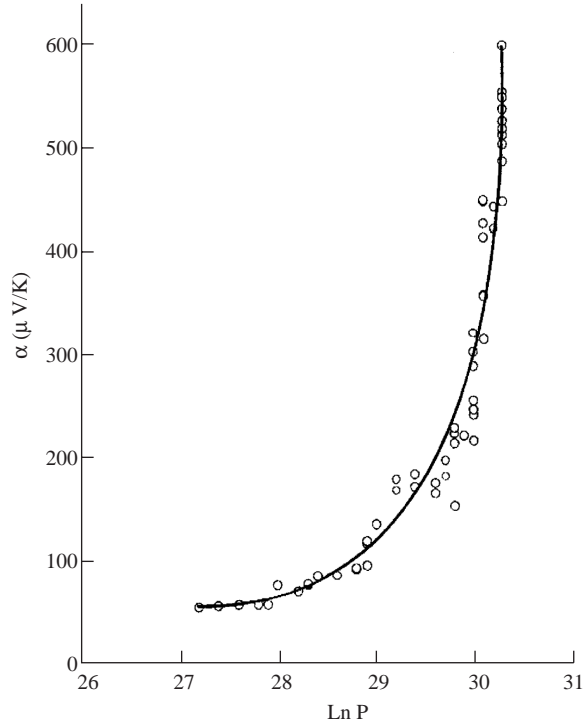


Figure 6. Relation between α and holes concentration of GaTe single crystal.

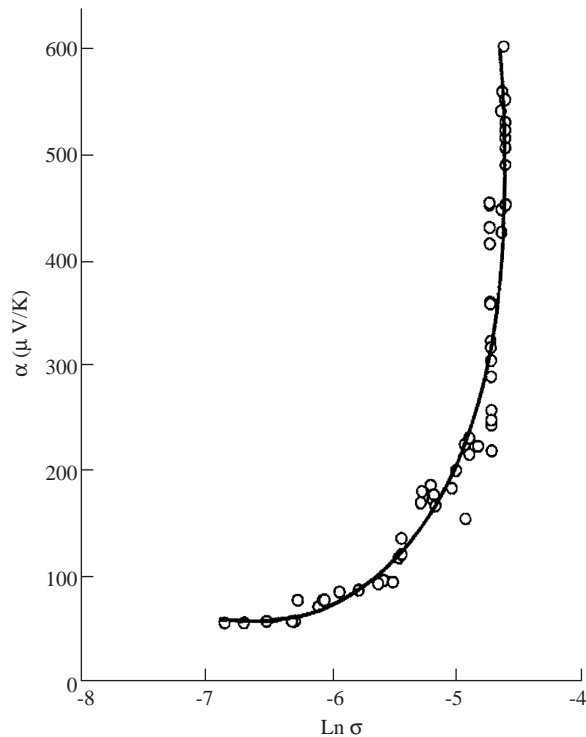


Figure 7. Variation of thermoelectric power with electrical conductivity for GaTe single crystal.

References

- [1] A. Koma and J. Yoshimura, *J. surf. Science*, **174**, (1986), 556.
- [2] N. Teraguchi, F. Kato, M. Konagai and K. Takahashi, *J. Electron. Mater.*, **20**, (1991), 247.
- [3] A. Mueller, W. Hoyer, E. Thomas, M. Wobst, *Phys. Stat. Sol. (a)*, **84**, (1984), K 97.
- [4] J. Rigoult and A. Rimsky, *Acta Cryst. B*, **36**, (1980), 416.
- [5] U. Schwarz, K. Syassen and R. Kniep, *J. Alloys and compounds*, **224**, (1995), 212.
- [6] C. Manfredotti, R. Murri, A. Rizzo, L. Vasanelli and G. Micocci, *Phys. Stat. Sol. A*, **29**, (1975), 475.
- [7] G. H. Souad, Ph.D Thesis, Faculty of Science (Aswan), Assuit University, Egypt, (1992).
- [8] G. A. Gamal, M. M. Nassary, S. A. Hussein, A. T. Nagat, *Cryst. Res. Technol*, **27**, 5, (1992), 629.
- [9] S. Pal, D. N. Bose, *Solid State Commun. (USA)*, **97**, 8, (1996), 725.
- [10] S. Pal, D. N. Bose, *Philosophical Magazin B*, **75**, 2, (1997), 311.
- [11] Bahattin Abay, Hassan Efeoglu, *Turk J. Phys*, **25**, (2001), 523.
- [12] J. Camasel, P. Merle and H. Mathieu, *Physica B*, **99**, (1980), 309.
- [13] K. Jezierski, *Opt. Appl*, **14**, 4, (1984), 529.
- [14] R. Girlanda, V. Grasso, G. Mondio and E. Doni, *Solid State Commun.* **57**, 4, (1986), 253.
- [15] J. F. Sanchez-Royo, A. Segura and V. Munoz, *Phys. Stat. Sol (a)*, **151**, (1995), 257.
- [16] M. Abdel Rahman, A. E. Belal, *J. Physics and Chemistry of Solids*, **61**, (2000), 925.

NASSARY

- [17] R. M. C, R. Pareje, A. Segura, V. Munoz and A. Chevy, *J. Phys: Condens. Matter*, **5**, (1993), 971.
- [18] J. Pellicer-Porres, A. Segura, A. San Miguel and V. Munoz, *Phys. Stat. Sol (b)*, **211**, (1998), 389.
- [19] H. S. Guder, B. Abay, H. Efeoglu, Y. K. Yogurtcu., *Journal of Luminescence*, **93**, 243–248, (2001).
- [20] M. M. Nassary, M. K. Gerges, H. T. Shaban, A. S. Salwa, *Physica B*, **337**, (2003), 130-137.
- [21] Hiroaki Okamoto, P. R. Subramanian and Linda Kacprzak, *Binary Alloy Phase Diagrams. ASM International* (1996).
- [22] S. A. Hussein, *Cryst. Res. Technol*, **24**, 6, (1989), 635.
- [23] E. Buratini, M. Grandolfo and C. Ranghiasi, *Phys. Rev. B*, **12**, 2, (1975), 664.
- [24] J. Lauc, *J. Phys. Rev.*, **95**, (1954), 1394.
- [25] A. H. Wilson, *Theory of Metals*, 2nd ed., University Press, Cambridge (1953).
- [26] P. H. E. Schmid and E. Mooser, *Helv. Phys. Acta.*, **45**, (1972), 870.